Molecular Crystals and Liquid Crystals
Publication details, including instructions for authors and subscription information:
http://www.informaworld.com/smpp/title~content=t713644168

Influence of the Physical Properties of Ferroelectric Liquid-Crystal Mixtures on the Photorefractive Effect

Atsushi Katsuragi[a]; Tatsuya Abe[a]; Hiroshi Endo[a]; Takeo Sasaki[a]
[a] Department of Chemistry, Faculty of Science, Tokyo University of Science, Shinjuku-ku, Tokyo, Japan

First published on: 14 December 2010

To cite this Article Katsuragi, Atsushi , Abe, Tatsuya , Endo, Hiroshi and Sasaki, Takeo(2010) 'Influence of the Physical Properties of Ferroelectric Liquid-Crystal Mixtures on the Photorefractive Effect', Molecular Crystals and Liquid Crystals, 533: 1, 27 — 41
To link to this Article: DOI: 10.1080/15421406.2010.526515
URL: http://dx.doi.org/10.1080/15421406.2010.526515

Mol. Cryst. Liq. Cryst., Vol. 533: pp. 27–41, 2010

ISSN: 1542-1406 print/1563-5287 online
DOI: 10.1080/15421406.2010.526515

Taylor & Francis
Taylor & Francis Group

Influence of the Physical Properties of Ferroelectric Liquid-Crystal Mixtures on the Photorefractive Effect

ATSUSHI KATSURAGI, TATSUYA ABE, HIROSHI ENDO, AND TAKEO SASAKI

Department of Chemistry, Faculty of Science, Tokyo University of Science, Shinjuku-ku, Tokyo, Japan

The relationship between the thermal properties and the photorefractive effect of various ferroelectric liquid-crystal compositions was investigated. Mixtures of phenyl pirimidine derivatives were used as host liquid-crystal materials to which chiral dopants and photoconductive compounds were added. The photorefractive two-beam coupling gain coefficient was strongly dependent on the magnitude of spontaneous polarization and the uniformity of the surface-stabilized state.

Keywords Ferroelectric liquid crystals; photorefractive effect; rotational viscosity; spontaneous polarization; surface-stabilized state

Introduction

The photorefractive effect is a phenomenon in which the refractive index of a material is modulated by the illumination of light [1–5]. The interference of two laser beams within a photorefractive material induces the generation of positive and negative charges at the bright positions in the interference fringe. The resultant charges move through the material by drift and/or diffusion processes. The mobilities of the positive and the negative charges are different in organic materials, so that the distribution of positive and negative charges are separated within the material. The bright and dark positions of the interference fringe are charged at opposite polarities to each other. This charge redistribution results in the formation of a space-charge field (internal electric field). The internal electric field induces the change in refractive index of the area between the bright and the dark positions through the electro-optic effect; therefore, the phase of the refractive index grating is shifted with respect to the interference fringe (Fig. 1). The phase-shifted grating gives rise to a phenomenon termed *asymmetric energy exchange in two-beam coupling* (2BC). The transmitted intensity of one of the interfering beams through the sample increases, whereas that of the other beam decreases.

Address correspondence to Takeo Sasaki, Department of Chemistry, Faculty of Science, Tokyo University of Science, 1-3 Kagurazaka, Shinjuku-ku, Tokyo 162-8601, Japan. E-mail: sasaki@rs.kagu.tus.ac.jp

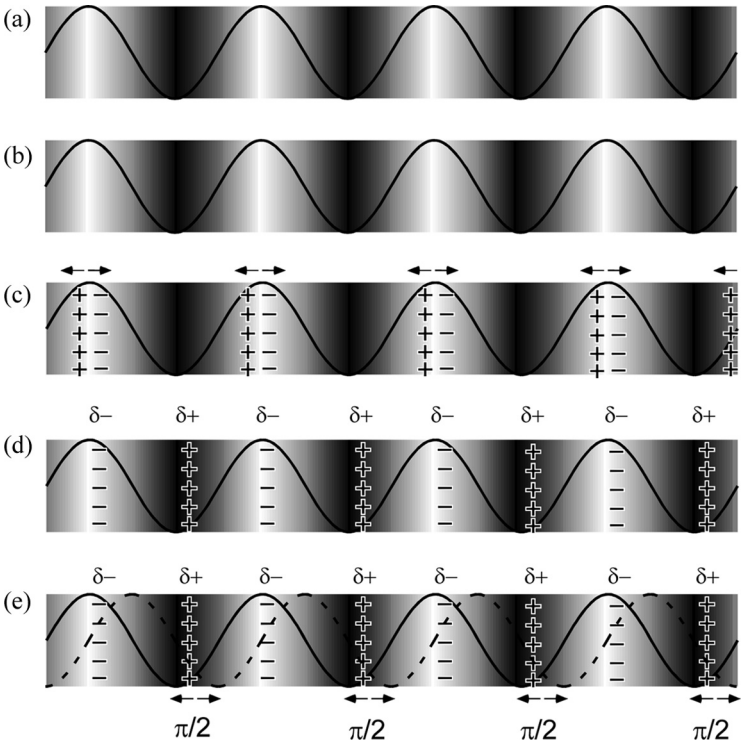

Figure 1. Schematic illustration of the photorefractive effect mechanism: (a) two laser beams interfere in the photorefractive material; (b) charge generation occurs in the bright areas of the interference fringes; (c) photogenerated charges are separated by diffusion in the presence of an external field; (d) an internal electric field is generated between the bright and dark positions due to the difference in the mobilities of the positive and the negative charges; (e) change in the refractive index is induced by the internal electric field, thereby generating a refractive index grating shifted with respect to the interference fringe.

Recently, the photorefractive effect in ferroelectric liquid crystals (FLCs) has been investigated [6–9] and is based on the response of spontaneous polarization (bulk polarization), which distinguishes it from other photorefractive materials in which the dipole moments of composite molecules respond to an internal electric field. FLCs are liquid crystals (LCs) that exhibit the chiral smectic C (SmC^*) phase [10,11]. The SmC^* phase in nature is characterized by a helical structure. When the FLC is sandwiched between glass plates to form a 2–10 μm-thick film, the helical structure unwinds and the surface-stabilized state (SS-state) appears. It should be noted here that the ferroelectricity of FLCs basically appears only in the SS-state.

In the SS-state of FLCs doped with photoconductive compounds, the interference of two laser beams induces an internal electric field and a grating based on the change in the direction of the spontaneous polarization (*Ps*) is produced at the interference fringe. A refractive index grating formation time of 20 ms was reported in an FLC doped with a photoconductive compound and a sensitizer [7,9]. In the present study, we have prepared FLCs with various physical properties and investigated the correlation between their physical properties and the photorefractive effect.

Experimental

Preparation of Ferroelectric Liquid-Crystal Mixtures

Four types of LCs that possess the phenyl pyrimidine structure (Fig. 2a) were obtained from Wako Chemicals Co. The phase transition temperatures of the LCs are listed in Table 1. 8.8PP, which exhibits the LC phase over the widest temperature range among the compounds used in this study, was mixed with the other LCs to prepare binary mixtures (8.8PP-8.6PP, 8.8PP-8.10PP, and 8.8PP-8.12PP). A 1:1 mixture of 8.8PP, and 8.10PP exhibited the smectic C phase (SmC) over the widest temperature; therefore, this mixture was selected as the base LC. In order to impart ferroelectricity to the LC, four types of chiral dopants (Fig. 2b) were mixed with the LC binary mixtures. Furthermore, two types of viscosity adjusters (Fig. 2c) were mixed with the base FLC. A photoconductive compound, CDH (1.0 wt%), and a sensitizer, TNF (0.1 wt%), were doped into the prepared FLC mixture (base FLC). The phase transition temperatures of the mixed samples were measured using

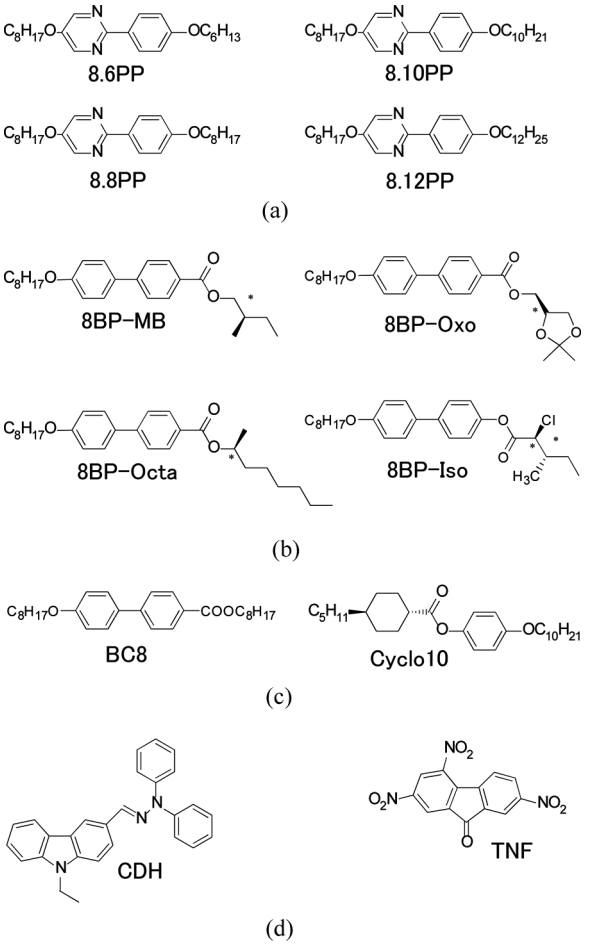

Figure 2. Structures of (a) LCs with phenyl pyrimidine structure, (b) chiral dopants, (c) viscosity adjusters, and the (d) photoconductive compound (CDH) and photosensitizer (TNF).

Table 1. Phase Transition Temperatures of Phenyl Pyrimidine LCs used in This Study

	Phase transition temperature[a] (°C)								
8.6PP	Cry	27.5	SmC	44.5	SmA	57.5	N	65.5	I
8.8PP	Cry	28.5	SmC	55.5	SmA	62.0	N	68.0	I
8.10PP	Cry	32.0	SmC	59.5	SmA	65.5	N	69.5	I
8.12PP	Cry	42.0	SmC	61.5	SmA	68.5	N	70.0	I

[a]Phases: Cry, crystal; SmC, smectic C; SmA, smectic A; N, nematic; I, isotropic.

differential scanning calorimetry (DSC) and polarizing optical microscopy (POM). The sample was injected into a sandwich glass cell equipped with 1 cm^2 indium tin oxide (ITO) electrodes and a polyimide alignment layer (LX-1400, Hitachi Chemicals Co.). The gap of the cell was 10 μm, as determined by a glass spacer. In order to align the LC molecules homogeneously, the sample was heated to the isotropic phase temperature and then cooled to room temperature at a rate of 0.5°C/min.

Measurements

The texture of the FLC sample was observed under a polarizing optical microscope (Olympus, BX-50, Mettler FP-80 and FP-82 hot stages). The spontaneous polarization of the FLC samples was measured using the triangular waveform voltage method (10 $V_{p\text{-}p}$, 100 Hz). The electro-optical switching time $T_{10\text{–}90}$ of the FLC samples was measured using a polarizing optical microscope with application of a

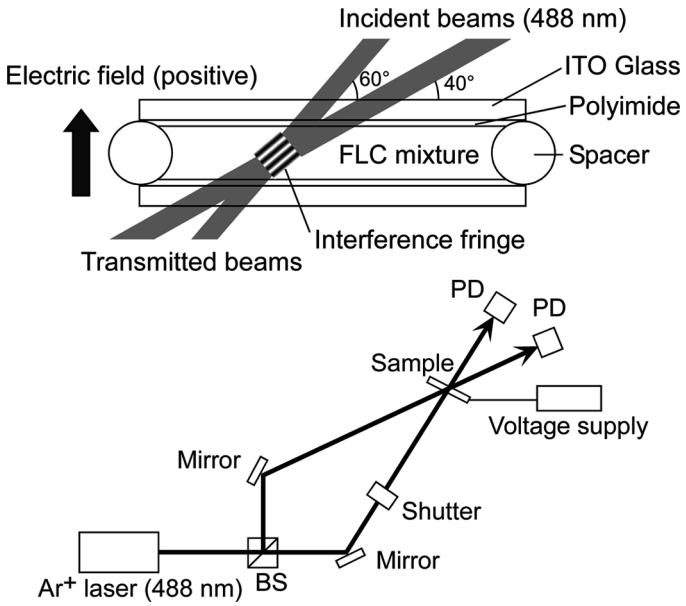

Figure 3. Schematic illustration of the 2BC experimental setup.

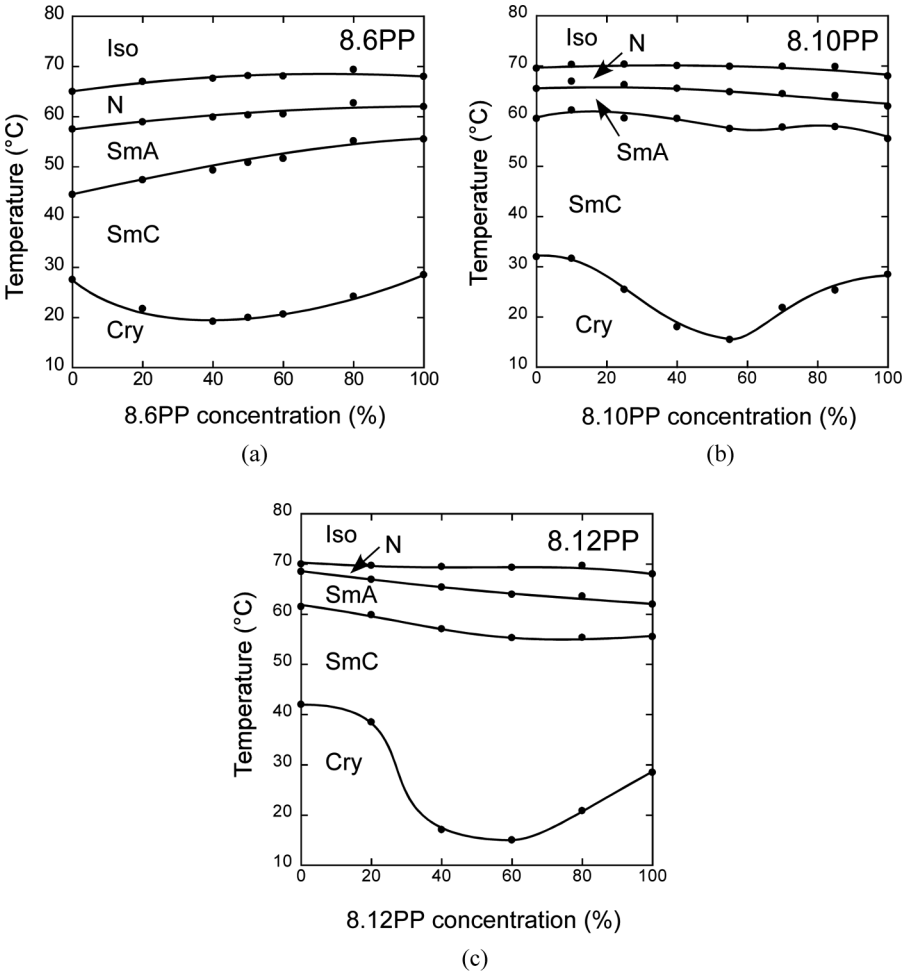

Figure 4. Phase diagrams of the binary LC mixtures of (a) 8.6PP/8.8PP, (b) 8.10PP/8.8PP, and (c) 8.12PP/8.8PP.

10 $V_{p\text{-}p}$ square-waveform voltage. The rotational viscosities of the FLC samples were calculated using the following equation:

$$T_{10-90} = \frac{1.75\eta}{PsE}$$

where η is the rotational viscosity, and E is the applied electric field. The photorefractivity was measured by a 2BC experiment. A p-polarized Ar^+ laser (Laser Graphics, 165LGS-S, 488 nm, continuous wave, 2.5 mW, 1 mm diameter) was used as a light source. The setup for the 2BC experiment is shown in Fig. 3. The incident angles of the beam to the glass plane were 40 and 60°. The interval of the interference fringe Λ was 1.69 μm. The photorefractive effects were measured with application of a DC voltage to the sample.

Results and Discussion

Effect of the FLC Mixture Composition on the SS-State

Binary mixtures of 8.8PP with 8.6PP, 8.10PP and 8.12PP were prepared and the phase diagrams of these mixtures are shown in Fig. 4. In order to obtain ferroelectricity, four types of chiral dopants were mixed with the base LC. The phase diagrams of the chiral dopant/base FLC mixtures are shown in Fig. 5. For the 8BP-MB, 8BP-Octa, and 8BP-Oxo chiral dopants, the temperature range of the smectic A phase (SmA) was expanded and that of the chiral nematic phase (N*) was reduced as the concentration of the chiral dopants was increased. A mixture of the base LC and 8BP-Iso exhibited the SmC* phase over the widest temperature range. The textures of the FLC mixtures with 10 wt% chiral dopant were observed under a POM. Many defects were observed in the texture of 8BP-MB, 8BP-Octa,

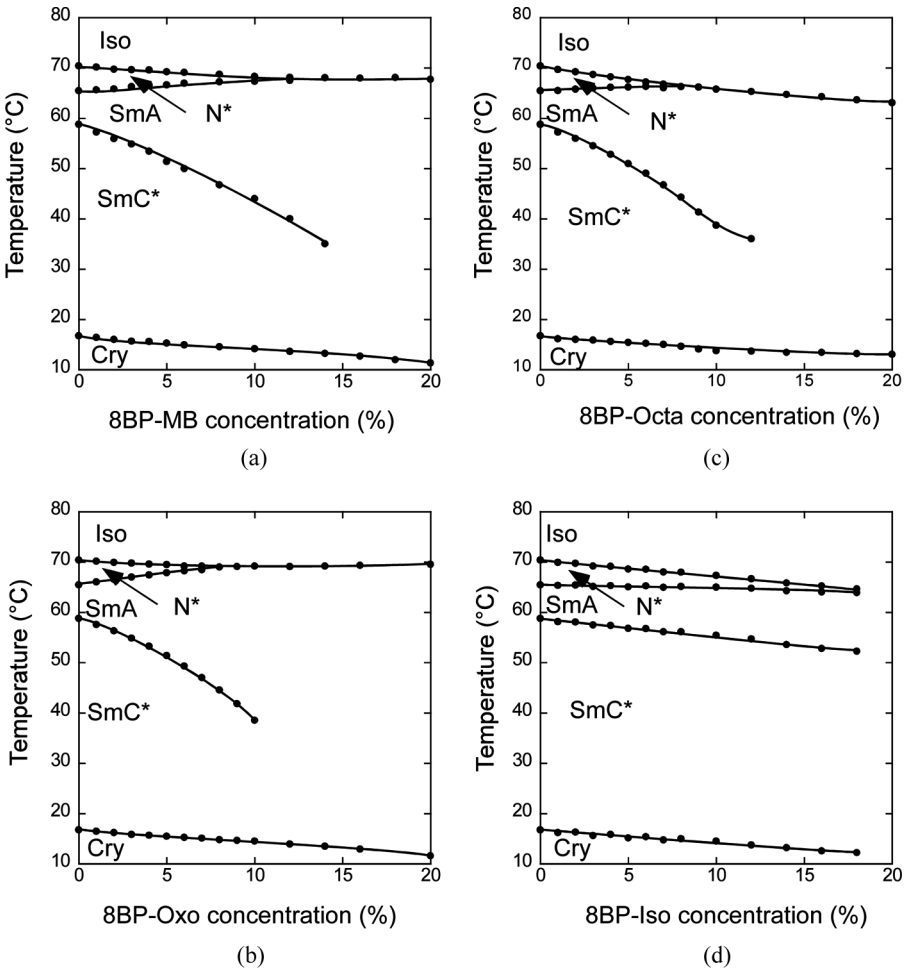

Figure 5. Phase diagrams of the mixtures of chiral dopants and the base LC (8.8PP/8.10PP, 1:1): (a) 8BP-MB/base-LC, (b) 8BP-Oxo/base-LC, (c) 8BP-Octa/base-LC, and (d) 8BP-Iso/base-LC.

and 8BP-Oxo. In contrast, very few defects were observed in the texture of 8BP-Iso. The 8BP-Iso molecule has a strong polar group and exhibits the SmC* phase; therefore, it is highly soluble in the base LC and maintains the phase transition sequence (crystal (Cry), SmC*, SmA, N*, isotropic (Iso)). The dependence of the magnitude of the *Ps* of the FLC mixtures on the chiral dopant concentration is shown in Fig. 6. The FLC mixture doped with 8BP-MB showed almost no *Ps* and the mixture with 8BP-Octa and 8BP-Oxo showed small *Ps* at concentrations higher than 6 wt%. On the other hand, the FLC mixture doped with 8BP-Iso had a *Ps* of 35 nC/cm^2 at 18 wt% concentration. The dependence of the electro-optical switching time of the FLC mixtures on the chiral dopant concentration is shown in Fig. 7. The FLC mixture doped with 8BP-MB did not respond to an applied field. When 8BP-Octa and 8BP-Oxo were used as the chiral dopants, the switching time was shortened with increasing concentration of the chiral dopant and reached approximately 600 μs. However, when 8BP-Iso was used as the chiral dopant, the switching time was

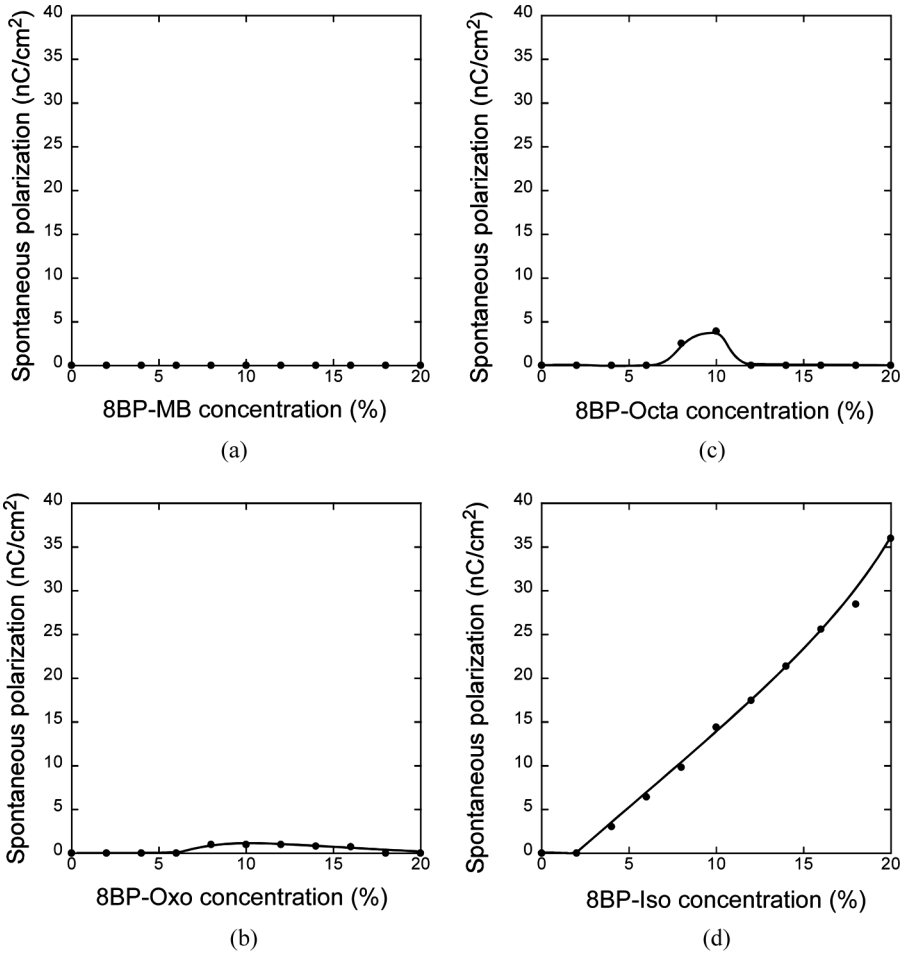

Figure 6. Dependence of the *Ps* magnitude on the chiral dopant concentration in the base LC (8.8PP/8.10PP, 1:1): (a) 8BP-MB/base-LC, (b) 8BP-Oxo/base-LC, (c) 8BP-Octa/base-LC, and (d) 8BP-Iso/base-LC.

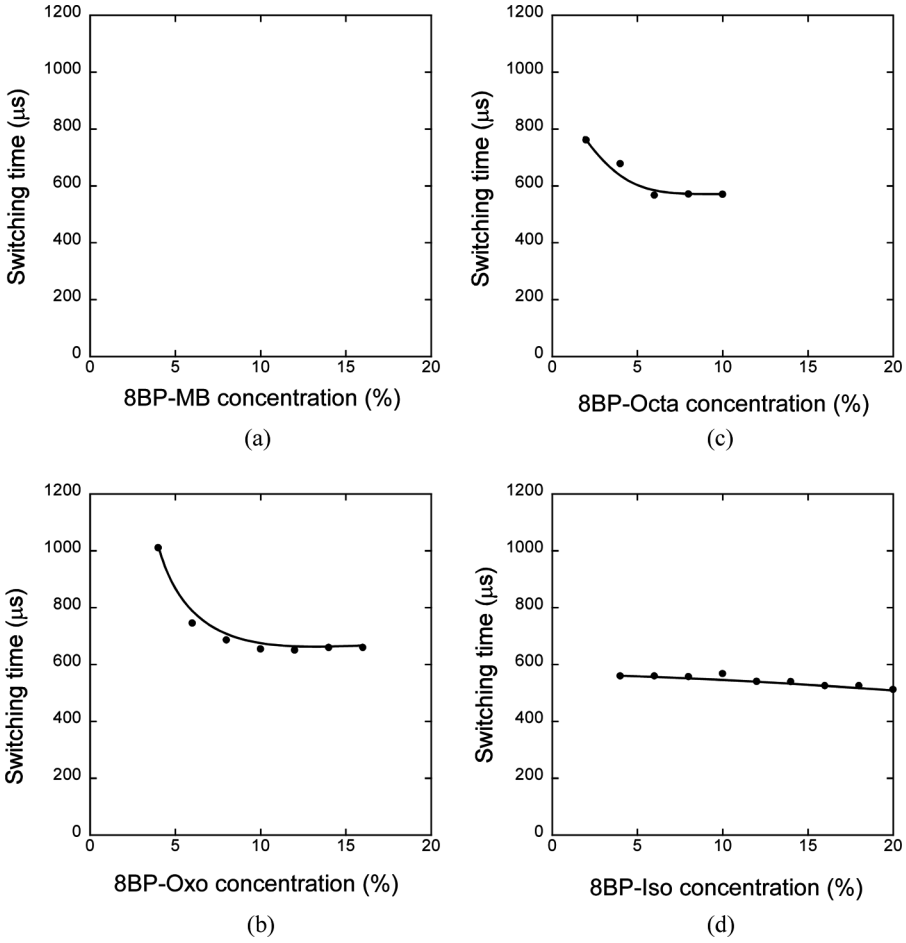

Figure 7. Dependence of the electro-optical switching time on the concentration of the chiral dopants in the base LC (8.8PP/8.10PP, 1:1): (a) 8BP-MB/base-LC, (b) 8BP-Oxo/base-LC, (c) 8BP-Octa/base-LC, and (d) 8BP-Iso/base-LC.

independent of the chiral dopant concentration and a switching time of 550 μs was obtained. It was considered that because the viscosity of the mixture was increased with the increase in the magnitude of the *Ps*, the switching acceleration was also canceled due to the increase in *Ps*. In order to obtain FLCs with highly uniform SS-state, Cyclo10 and BC8 were also mixed with the base FLC. For photorefractive measurement, the concentration of Cyclo10 was set to 10 wt%, and that of BC8 to 4 wt%. In addition, the photoconductive compound CDH (1 wt%) and sensitizer TNF (0.1 wt%) were mixed with the base FLC to obtain a photorefractive FLC (PR-FLC).

Effect of the Viscosity Adjuster on the Homogeneity of the SS-State

The effect of the Cyclo10 concentration on the homogeneity of the SS-state was investigated. The phase diagram for the FLC sample is shown in Fig. 8. The phase

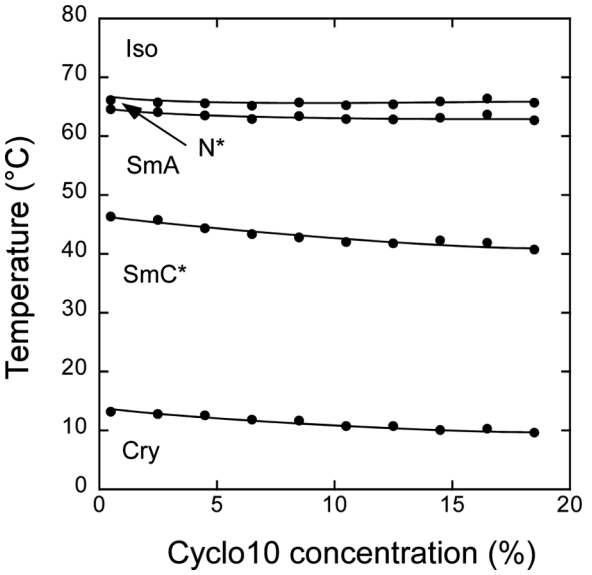

Figure 8. Phase diagram of the PR-FLC mixture (8.8PP, 43 wt%; 8.10PP, 43 wt%; BC8, 4 wt%; and 8BP-Iso, 10 wt%) and Cyclo10.

transition sequence (Cry, SmC*, SmA, N*, Iso) was retained even if Cyclo10 was mixed with the base FLC at a concentration of 20 wt%. The textures of the PR-FLCs sample observed by POM are shown in Fig. 9. Many defects were observed in the textures of the low Cyclo10 concentration samples; however, as the Cyclo10 concentration was increased, a highly homogeneous SS-state was obtained. It was considered that the introduction of Cyclo10 increased the miscibility of the photoconductive compounds CDH/TNF.

Spontaneous Polarization and Switching Response of the FLC Mixtures

The magnitude of the *Ps* was decreased with increasing concentration of the Cyclo10, as shown in Fig. 10. The switching time was almost independent of the Cyclo10 concentration, as shown in Fig. 11. It was considered that although the *Ps* was reduced by the increase in the Cyclo10 concentration, the viscosity of the FLC mixture was also reduced and the effects of both on the switching time were canceled.

Photorefractivity of the FLC Mixtures

The photorefractive effect of the PR-FLC samples was evaluated by a 2BC experiment (Fig. 3). The diffraction condition was evaluated using the nondimensional parameter Q [1–5].

$$Q = \frac{2\pi\lambda D}{n\Lambda^2}$$

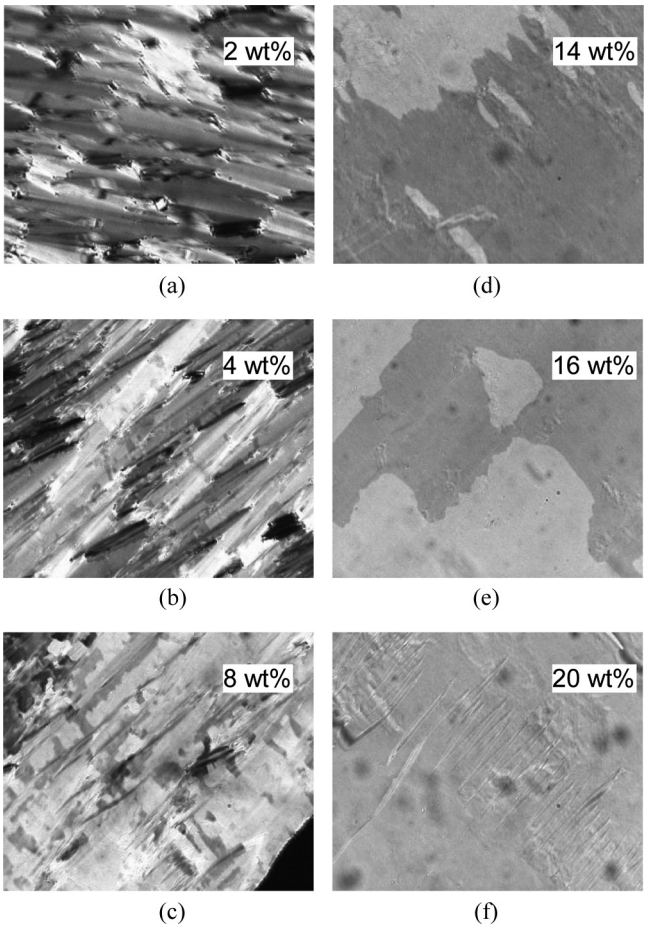

Figure 9. Texture observed in the SS-state of the PR-FLC mixture doped with (a) 2, (b) 4, (c) 8, (d) 14, (e) 16, and (f) 20 wt% Cyclo10. The PR-FLC was a mixture of the base FLC (8.8PP, 43 wt%; 8.10PP, 43 wt%; BC8, 4 wt%; and 8BP-Iso, 10 wt%) doped with CDH (1 wt%) and TNF (0.1 wt%). The gap of the LC-cell was 10 μm.

where D is the interaction path length for the signal beam. The Bragg regime of optical diffraction is defined as $Q > 1$. Conversely, $Q < 1$ is defined as the Raman-Nath regime of optical diffraction. A Q value greater than 10 is usually required to guarantee the occurrence of diffraction entirely in the Bragg regime. Under the experimental conditions shown in Fig. 3, the Q parameter was calculated to be 6–8. Therefore, the diffraction in the Bragg regime is predominant but also includes a small Raman-Nath component. The photorefractive effect was measured with application of a *DC* voltage. The external electric field was applied in order to increase the charge separation efficiency. A typical example of the 2BC signal is shown in Fig. 12. A signal beam and a pump beam were allowed to interfere in the sample. The intensity of one transmitted beam was increased, whereas that of the other was decreased; the changes were completely symmetric, which indicates asymmetric energy exchange of the two beams. The magnitude of the photorefractive effect was estimated from the gain coefficient,

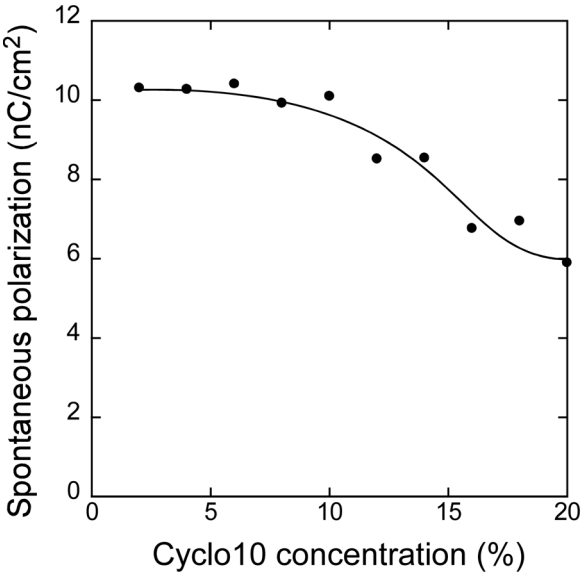

Figure 10. Dependence of the *Ps* magnitude on the concentration of Cyclo10 in the PR-FLC mixture measured at 30°C. The PR-FLC was a mixture of the base-FLC (8.8PP, 43 wt%; 8.10PP, 43 wt%; BC8, 4 wt%; and 8BP-Iso, 10 wt%) doped with CDH (1 wt%) and TNF (0.1 wt%). The gap of the LC-cell was 2 μm.

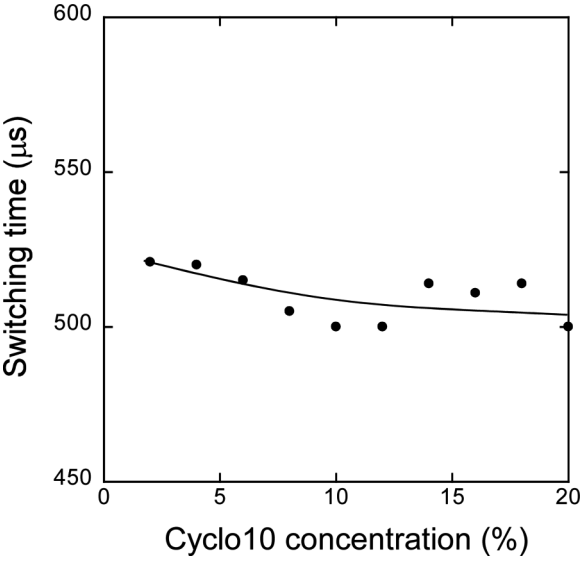

Figure 11. Dependence of the electro-optical switching time on the concentration of Cyclo10 in the PR-FLC measured at 30°C. The PR-FLC was a mixture of the base-FLC (8.8PP, 43 wt%; 8.10PP, 43 wt%; BC8, 4 wt%; and 8BP-Iso, 10 wt%) doped with CDH (1 wt%) and TNF (0.1 wt%). The gap of the LC-cell was 2 μm.

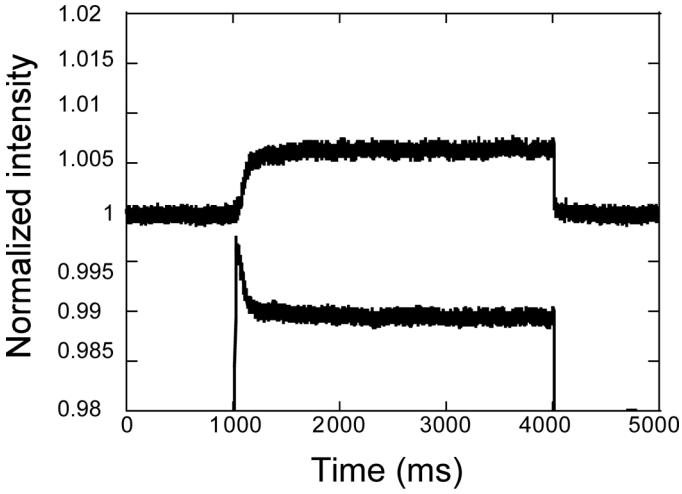

Figure 12. Typical example of asymmetric energy exchange observed in the 2BC experiment with the PR-FLC sample at 30°C. The sample used was a mixture of base FLC (8.8PP, 38.7 wt%; 8.10PP, 38.7 wt%; BC8, 3.6 wt%; Cyclo10, 9 wt%; and 8BP-Iso, 10 wt%) doped with CDH (1 wt%) and TNF (0.1 wt%).

which was calculated using the following equation:

$$\Gamma = \frac{1}{D}\ln\left(\frac{gm}{1+m-g}\right)$$

where m is the ratio of the intensities of the beam (pump/signal) in front of the sample, and g is the ratio of the intensities of the signal beam (with pump/without pump) behind the sample. The photorefractive effect occurred in all samples used in this study. The clarity of the SS-state is very important for the photorefractive effect in FLCs. The dependence of the 2BC gain coefficient on the applied electric field is shown in Fig. 13. The gain coefficient increased with the magnitude of the applied

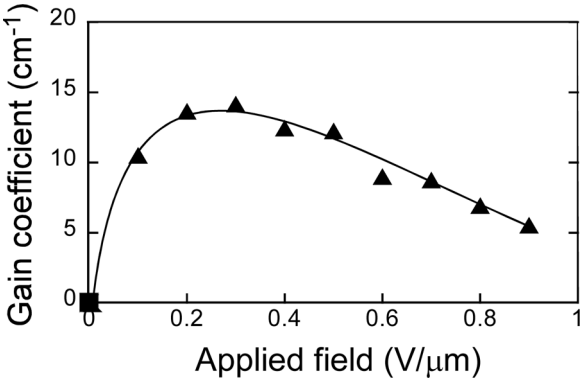

Figure 13. Magnitude of the gain coefficient as a function of the applied electric field. The sample used was a mixture of base FLC (8.8PP, 38.7 wt%; 8.10PP, 38.7 wt%; BC8, 3.6 wt%; Cyclo10, 9 wt%; and 8BP-Iso, 10 wt%) doped with CDH (1 wt%) and TNF (0.1 wt%).

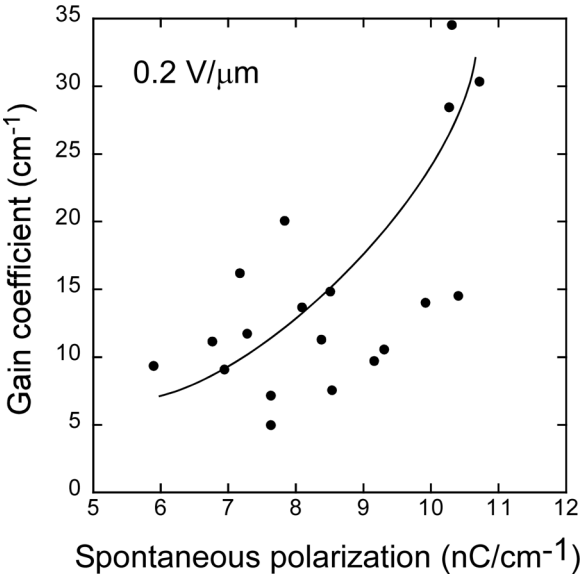

Figure 14. Dependence of the gain coefficient on the magnitude of *Ps*. The sample used was a mixture of base FLC (8.8PP, 38.7 wt%; 8.10PP, 38.7 wt%; BC8, 3.6 wt%; Cyclo10, 9 wt%; and 8BP-Iso, 10 wt%) doped with CDH (1 wt%) and TNF (0.1 wt%). The gain coefficient was measured with application of an external electric field at 0.2 V/μm.

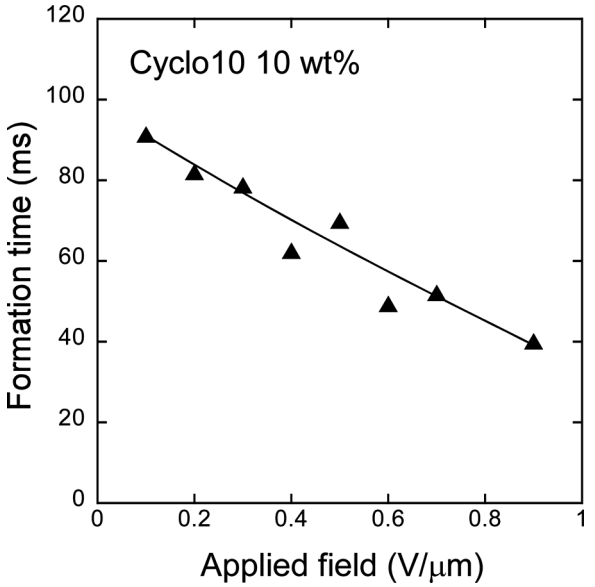

Figure 15. Dependence of the refractive index grating formation time as a function of the external electric field measured at 30°C. The concentration of Cyclo10 was varied from 2.0 to 20.0 wt%. The sample used was a mixture of base FLC (8.8PP, 38.7 wt%; 8.10PP, 38.7 wt%;, BC8, 3.6 wt%; Cyclo10, 9 wt%; and 8BP-Iso, 10 wt%) doped with CDH (1 wt%) and TNF (0.1 wt%).

electric field up to 0.2 V/μm due to the increased efficiency of the charge separation. The gain coefficient took a maximum value at around 0.2 V/μm; however, when the electric field was increased above 0.2 V/μm, its magnitude decreased. A large external field impedes the change in the *Ps* direction. The magnitude of the gain coefficients tend to increase with the magnitude of *Ps*, as shown in Fig. 14.

Refractive Index Grating Formation Time

The refractive index grating formation time (response time) was measured. The 2BC coupling signal was fitted by the following equation:

$$r(t) = r\left[1 - \exp\left\{\frac{t}{\tau}\right\}\right]^2$$

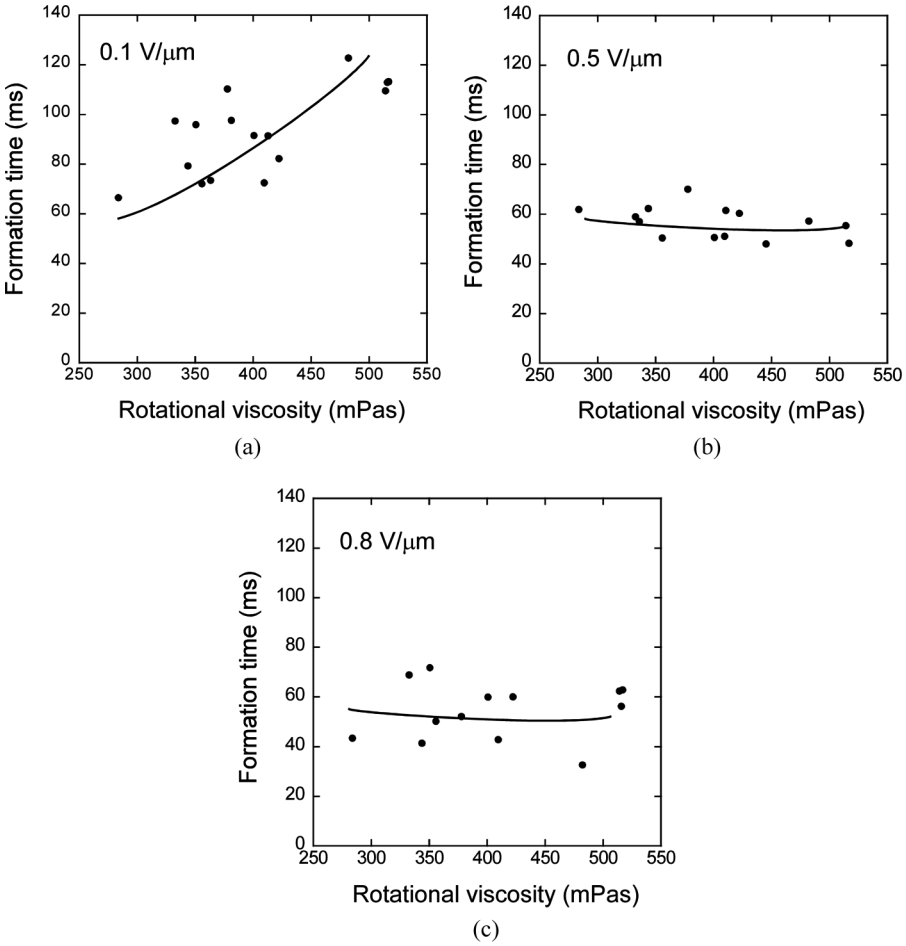

Figure 16. Refractive index grating formation time as a function of the rotational viscosity measured with application of (a) 0.1, (b) 0.5, and (c) 0.8 V/μm. The sample used was a mixture of base FLC (8.8PP, 38.7 wt%; 8.10PP, 38.7 wt%; BC8, 3.6 wt%; Cyclo10, 9 wt%; and 8BP-Iso, 10 wt%) doped with CDH (1 wt%) and TNF (0.1 wt%).

The dependence of the formation time on the applied electric field is shown in Fig. 15. The formation time becomes faster as the applied electric field is increased. A formation time of 40 ms was obtained under an applied field of 0.9 V/μm for the sample doped with 10 wt% Cyclo10. The dependence of the formation time on the rotational viscosity is shown in Fig. 16. Under a low applied field of 0.1 V/μm, the formation time was proportional to the rotational viscosity. However, under a high applied field, such as 0.5 and 0.8 V/μm, the formation time was not proportional to the rotational viscosity. It is considered that two elements affect the formation time: the external field and the viscosity of the medium. An increase in the external field results in an increase in the efficiency of the charge separation and a change in the *Ps* direction is easier in a low-viscosity medium than in a high-viscosity medium. Under a low external applied field, the charge separation efficiency is small, which leads to a smaller internal electric field. In this case, the viscosity of the LC has a significant influence on the formation of the refractive index grating, based on the change in the *Ps* direction. On the other hand, under a high external electric field, the internal electric field is sufficiently large, so that the decrease in viscosity does not affect the refractive index formation time.

Conclusion

FLC mixtures with various compositions were prepared and the influence of their physical properties on the photorefractive effect was investigated. The 2BC gain coefficients were larger in FLC mixtures that form a uniform, defect-free SS-state. Both the gain coefficient and response time were found to be strongly dependent on the magnitude of *Ps* and the rotational viscosity of the FLC.

Acknowledgment

The authors thank the Cannon Foundation for financial support.

References

[1] Yeh, P. (1993). *Introduction to Photorefractive Nonlinear Optics*, John Wiley & Sons: New York.
[2] Moerner, W. E., & Silence, S. M. (1994). *Chem. Rev.*, *94*, 127.
[3] Feinberg, J. (1983). *Optical Phase Conjugation*, Fisher, R. A. (Ed.), Academic Press: New York, 417–443.
[4] Günter, P., & Huignard, J. P. (Eds.) (1988). *Photorefractive Materials and Their Applications I & II*, Springer Verlag: Berlin.
[5] Solymar, L., Webb, D. J., & Grunnet-Jepsen, A. (1996). *The Physics and Applications of Photorefractive Materials*, Oxford: New York.
[6] Sasaki, T., Kino, Y., Shibata, M., Mizusaki, N., Katsuragi, A., Ishikawa, Y., & Yoshimi, Y. (2001). *Appl. Phys. Lett.*, *78*, 4112.
[7] Sasaki, T., Katsuragi, A., Mochizuki, O., & Nakazawa, Y. (2003). *J. Phys. Chem. B*, *107*, 7659.
[8] Talarico, M., & Golemme, A. (2006). *Nat. Mater.*, *5*, 185.
[9] Moriya, N., & Sasaki, T. (2008). *Mol. Cryst. Liq. Cryst.*, *482*, 33.
[10] Fukuda, A., & Takezoe, H. (1990). *Structure and Properties of Ferroelectric Liquid Crystals*, Corona: Tokyo.
[11] Fukuda, A. (1992). *Ferroelectric Liquid Crystal Display and Material*, CMC: Tokyo.